Parasite-intrinsic factors can explain ordered progression of trypanosome antigenic variation

Katrina A. Lythgoe*, Liam J. Morrison†, Andrew F. Read*, and J. David Barry†‡

*Institutes of Evolution, Immunology, and Infection Research, School of Biological Sciences, University of Edinburgh, Edinburgh EH9 3JT, United Kingdom; and †Wellcome Centre for Molecular Parasitology, Glasgow Biomedical Research Centre, University of Glasgow, 120 University Place, Glasgow G12 8TA, United Kingdom

Edited by Robert May, University of Oxford, Oxford, United Kingdom, and approved March 21, 2007 (received for review July 21, 2006)

Pathogens often persist during infection because of antigenic variation in which they evade immunity by switching between distinct surface antigen variants. A central question is how ordered appearance of variants, an important determinant of chronicity, is achieved. Theories suggest that it results directly from a complex pattern of transition connectivity between variants or indirectly from effects such as immune cross-reactivity or differential variant growth rates. Using a mathematical model based only on known infection variables, we show that order in trypanosome infections can be explained more parsimoniously by a simpler combination of two key parasite-intrinsic factors: differential activation rates of parasite variant surface glycoprotein (VSG) genes and density-dependent parasite differentiation. The model outcomes concur with empirical evidence that several variants are expressed simultaneously and that parasitaemia peaks correlate with *VSG* genes within distinct activation probability groups. Our findings provide a possible explanation for the enormity of the recently sequenced *VSG* silent archive and have important implications for field transmission.

mathematical model | *Typanosoma brucei* | variant surface glycoprotein | switching | hierarchy

Trypanosomes switch antigens primarily by duplication of *VSG*s, in which the new gene copy replaces the expressed *VSG*. There is a large archive of 1,500–2,000 silent *VSG*s from which to duplicate (1). The *VSG* group activated with highest frequency is telomere-proximal, and it is duplicated by way of homologous gene flanks. The second main group, located in subtelomeric arrays, is activated with relatively low frequency. This group is mostly composed of pseudogenes, gene fragments, or genes encoding dysfunctional variant surface glycoproteins (VSGs) (1) but can be expressed as mosaic genes through donation of segments of coding sequence from different *VSG*s (2). A fundamental difference between these two archive groups is that *VSG*s in the first switch independently of each other, duplicating by way of gene flanks, whereas the second group does not switch independently, because its duplication involves coding sequence homologies.

Order in VSG expression could be imposed by the parasite or by indirect influences. The most commonly proposed molecular basis for order (3–5) is that it operates through innate differences in the activation probability for *VSG*s, dependent on the flanking sequence homologies of the silent gene being activated or, for mosaic genes, degrees of homology between coding sequences of the incoming and outgoing *VSG* genes. Indeed, the bacterium *Anaplasma marginale*, using an archival system, achieves differential switching by way of homologies in both gene flank and coding sequences (6). There is empirical support for this general trypanosome molecular mechanism (7–14), and recent quantitative analysis has revealed a higher degree of order than previously supposed (15). Three studies in particular, together involving >100 variants in >50 infections, have firmly established order in *VSG* expression (15–17). Most studies, however, have involved only single relapses and therefore only a few high-probability switches, and it is important now to analyze long-term infection in greater detail to help ascertain the range and patterns of switch rates that can yield order and how ordered expression interacts with trypanosome growth variables to yield the characteristic fluctuating parasitemia. One way to do so is to use mathematical modeling on the basis of known, major variables in trypanosome growth and antigenic variation.

In contrast to the molecular hypothesis, most theoretical modeling studies have assumed a uniform switching pattern among variants (Fig. 1*A*) and invoked indirect effects to explain order. There is, however, little empirical support for these other factors. It has been proposed that order arises from variant-specific differences in intrinsic growth rates (18), but such an effect is, at best, insignificant (18, 19) and is not supported theoretically (20, 21). Another possibility, that order arises from differential efficiencies of variant-specific immune responses, is negated by the observation that different variants are cleared *in vivo* by the immune system with closely similar dynamics (22). The suggestion that transient expression of two VSGs by a trypanosome, such as during switching, could enhance sensitivity to antibodies and therefore influence order (21) is not supported by the normal *in vivo* growth and reduced immunogenicity of artificially created double expressors (23, 24). Antigenic "cross-reactivity" on the basis of common, invariant antigens (25, 26) is unlikely to cause order, because such molecules do not elicit protective responses against trypanosomes (27–29). Order generated through VSGs sharing epitopes, corresponding to what has been proposed for PfEMP1 switching in the malaria parasite *Plasmodium falciparum* (30), is highly unlikely, because the degree of order observed would require multiple VSG cross-reactions, but these have been seen only for products of highly related *VSG* genes, and in all cases cross-protection was complete (13, 31). The cross-reactivity model proposed for malaria (30) depends on transient antibody responses, but, within the limits of available tests, they have not been detected in studies of trypanosome infections (15–17, 32).

In light of the insights into the make-up of the *VSG* repertoire provided by the genome project (1) and, in particular, the emerging possibility that mosaic gene formation from pseudogenes makes a substantial contribution to antigenic variation, there is a requirement to revisit and substantially revise the existing modeling approaches to trypanosome VSG switching and, in particular, to include differential *VSG* activation rates analogous to those seen *in vivo*. Moreover, it is important to involve density-dependent parasite differentiation, a key growth

Author contributions: K.A.L., L.J.M., A.F.R., and J.D.B. designed research; K.A.L., L.J.M., A.F.R., and J.D.B. performed research; K.A.L. contributed new reagents/analytic tools; K.A.L., L.J.M., A.F.R., and J.D.B. analyzed data; and K.A.L., L.J.M., A.F.R., and J.D.B. wrote the paper.

The authors declare no conflict of interest.

This article is a PNAS Direct Submission.

Abbreviation: VSG, variant surface glycoprotein.

‡To whom correspondence should be addressed. E-mail: j.d.barry@bio.gla.ac.uk.

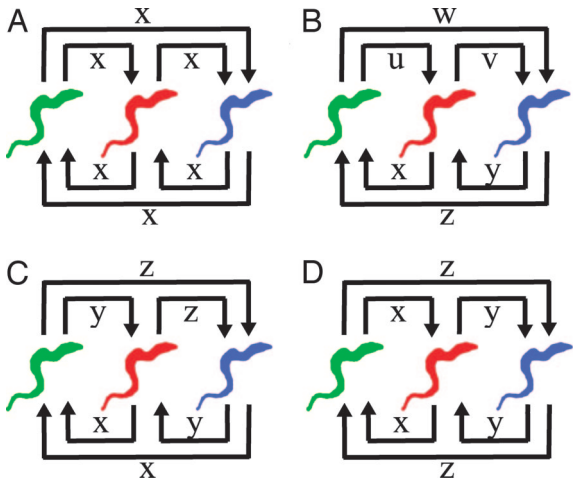

Fig. 1. Different suggested switching patterns. The green, red, and blue shapes represent trypanosomes expressing different *VSG* genes. The values *u*, *v*, *w*, *x*, *y*, and *z* represent switching rates. (*A*) Uniform switching pattern. All variants are switched to and from at the same rate. (*B*) Interdependent switching pattern associated with direction of switch. The rate to which a variant is switched depends on the variant from which it is switching. The rate depends on the direction of the switching so that, for example, the rate at which red switches to blue is not the same as the rate at which blue switches to red. This is the switching pattern used by Frank (35). (*C*) Differential activation switching pattern. Each variant has a distinct activation rate independent of the variant it is replacing so that, for example, the rate at which red switches to blue is equal to the rate at which green switches to blue. (*D*) Interdependent switching not associated with switch direction, as occurs in homology-dependent (mosaic) switching. The rate to which a variant is switched depends on the variant from which it was switched. The rate does not depend on the direction of switching so that, for example, the rate at which red switches to blue is equal to the rate at which blue switches to red.

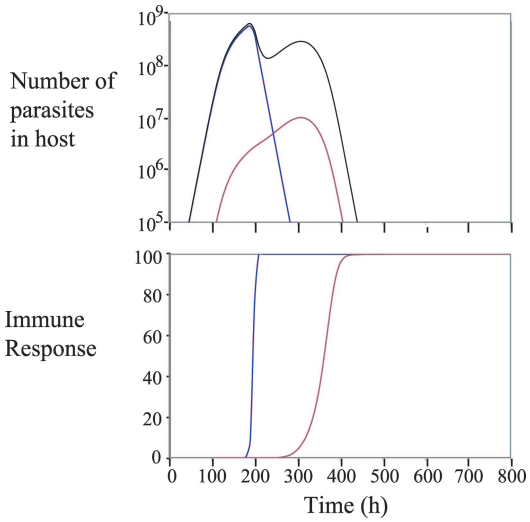

Fig. 2. Time series of parasite dynamics and the immune response with a uniform switching pattern. All variants have equal probability of switching to any other variant so that the probability that any parasite switches to another variant or that any variant is switched to is 0.01 per population doubling. (*Upper*) Shown are the parasite numbers. The black line represents the total number of parasites, and each colored line represents a variant. Only one line is visible because the trajectories of all but the inoculating variant overlap. (*Lower*) Shown is the immune response against each variant. Apart from the inoculating variant, the trajectories of the immune response against each of the variants are identical. The factors influencing growth are multiplication rate, nonspecific growth inhibition (37), switching between variants and the density-dependent variables of differentiation to the nonproliferating stumpy stage (33), immune response onset (46, 47), and removal of variants. The simulation began with 1,000 trypanosomes (akin to natural transmissions from tsetse) and involved a computationally feasible archive of 30 *VSGs*; the output provides a sample of events rather than simulating an entire infection. The parameters are as follows: $n = 30$; $r = 0.1\ h^{-1}$; $d = 0.5\ h^{-1}$; $\delta = 0.1\ h^{-1}$; $K = 1 \times 10^8$; $\rho = 2{,}500$; $c_i = 100$; $C = 1 \times 10^8$; and $x = 3$.

parameter (33, 34) not previously incorporated into antigenic variation models.

Of existing mathematical models, only one has addressed differential *VSG* activation rates, and it successfully simulated ordered expression (35). The model was based, however, on interdependent switching between variants, in which the probability of switching on a particular variant (activation probability) depends on the currently expressed variant (Fig. 1*B*) and is associated with the direction of the switch, such that the probability of switching from variant *i* to variant *j* will not equal the probability of switching from variant *j* to variant *i*. This assumption is not supported by empirical evidence that early switches are governed by the *VSG* being activated, rather than what is currently expressed (15), and that order early in infections is independent of the infecting variant (15–17, 22, 36).

Given these data, a more plausible model is a differential-activation switching pattern during the early stage of infection (Fig. 1*C*), in which each variant has a distinct activation rate, independent of the currently expressed variant. This pattern changes later in infection, when mosaic VSGs are expressed, because the involvement of coding sequence homology in switching means that the variant being switched to does depend on the variant currently being expressed (Fig. 1*D*).

Trypanosome survival and growth in mammalian hosts and the interplay between infection profile and antigenic variation are complex, and it is important to incorporate variables that have been demonstrated to influence parasitemia and to exclude those of little or no biological relevance. Factors known to exert significant influence on the course of infection include the density-dependent, parasite-triggered differentiation to the nondividing short stumpy stage (33, 34), density-dependent general growth interference between trypanosomes (37) (which is likely to include any indirect immune system effects, such as reported in model host infections; ref. 38), and the VSG-specific antibody responses. All these have been quantified experimentally, permitting inclusion in mathematical modeling.

Factors thought not to impact on the generation of ordered antigenic variation include dispersed anatomical location of trypanosomes within the host (39), infection-associated immunosuppression (40), and putative, direct-host involvement in the switching mechanism (17, 41). Ordered antigenic variation occurs in the bloodstream without complication from parasites in other anatomical niches. *Trypanosoma vivax* is mainly vascular yet displays order (17), and direct analysis of the distribution and exchange of *Trypanosoma brucei* variants between vascular and extravascular sites by using VSG-specific antibodies (39) has refuted the proposal from indirect studies that extravascular colonies seed the variant pool in the blood (42). It is clear from empirical analyses of >100 variants in >50 host animals that antibody responses against individual variants generally are very persistent, usually lasting for as long as infections are followed (15–17). These antibodies are trypanolytic and, consequently, once a variant has arisen it does not reappear in long-term infection (15–17). Hence, immunosuppressive effects reported in model hosts (40) are not relevant to antigenic variation, certainly up to the terminal stages of infection. There is another VSG-triggered immune response, which activates macrophages to yield trypanocidal agents (38), but it is not known whether this response kills trypanosomes variant-specifically. Because this response is mainly extravascular (43), and order is not influenced by trypanosomes in that compartment (17, 39), it is unlikely to

be of major influence on order. Although the antitrypanosome immune response is complex (38), the dynamics of antibody production and variant killing strongly correlate, and it is empirical data regarding antibody thresholds on which we base the model. Hosts are not directly involved in switching, which is parasite-intrinsic (41) and independent of host species (17); the host acts solely to select new variants by killing old ones.

Here, we have developed a mathematical model incorporating all of the influential parameters listed above. To examine how switch rates and patterns influence order and how order influences infection profile, initially we tested whether the differential-activation switching pattern (Fig. 1*C*) can yield the main elements of realistic infection profiles, then we extended our model to test the homology switching pattern for mosaic genes, hitherto unincorporated in any trypanosome model (Fig. 1*D*), but likely to be a major influence in chronic infections. Because other parameters have been quantified empirically, the only one varied in our model was the switch rate between variants. Hence, our model has the benefit of being more parsimonious and biologically more realistic than other models.

We imagined a population of trypanosomes in which the number of replicative (slender) and nonreplicative (stumpy, cell cycle arrested) trypanosomes that are variant i are given by v_i and m_i, respectively. The slender cells have an intrinsic growth rate r_t, where t is time after inoculation and, when a slender cell divides, there is a probability, f, that one daughter cell will differentiate to a stumpy cell. This rate of differentiation increases as the total number of parasites increases (33, 34). The slender cells are also able to switch VSG. We assumed that all variants switch off at the same rate, but there are differences in the activation rate of different *VSG*s. This switching rate we call $s_{i,j}$, which is the rate at which variant i is switched to from variant j. As the host acquires immunity to variant i, the slender and stumpy cells will be killed at a rate dependent on the strength of the acquired immune response, a_i. The value of a_i can range from 0 to 1, where 0 means no immune response and 1 means the maximum possible immune response. The maximum rates at which the immune system can kill the slender and stumpy cells are d and δ, respectively. It was computationally unfeasible to process the hundreds or more of possible variants, so in all simulations we included a *VSG* repertoire of 30. Although this clearly will abbreviate simulated infections, it will not influence what is being tested, the patterns of variants in peaks. The simulations were all initiated with a single variant, because that was the basis of almost all published empirical analyses of infections.

The dynamics of the slender and stumpy cells are given by the following:

$$\frac{dv_i}{dt} = v_i\, r_t\, (1 - f) - v_i\, da_i + \sum_{j=1}^{n} (v_j s_{i,j} - v_i s_{j,i}) \qquad [1]$$

$$\frac{dm_i}{dt} = v_i r_t f - m_i \delta a_i, \qquad [2]$$

where

$$f = 1 - e^{-(V+M)/K} \qquad [3]$$

and

$$r_t = re^{-t/\rho}. \qquad [4]$$

Here, V is the total number of slender cells in the host, M is the total number of stumpy cells, and K is the number of cells at which maximum stumpy production occurs. At the beginning of infection, the growth rate is at a maximum, r, but as the infection progresses, there is generalized inhibition of the growth rate independent of the acquired immune response to each of the variants (37). For all of our simulations, we chose a ρ value of 2,500 on the basis of the observation that it takes ≈26 days for growth to be inhibited by 50% (37). Other parameters used in all simulations are $n = 30$; $r = 0.1\ \text{h}^{-1}$ (44); $d = 0.5\ \text{h}^{-1}$; $\delta = 0.1\ \text{h}^{-1}$ (45); and $K = 1 \times 10^8$ (33).

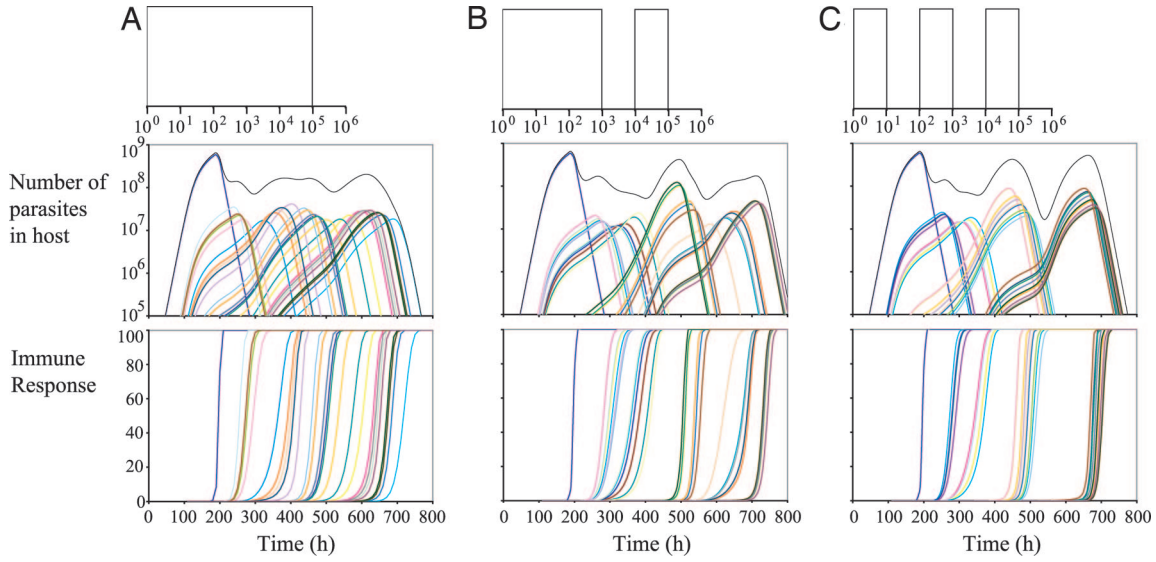

Fig. 3. Time series of parasite dynamics and the immune response with a differential-activation switching pattern. The rate at which a variant is switched to varies but is independent of which variant it is replacing. (*Top*) The bar graphs show the distribution from which the switching rates were chosen prior to the simulation. These rates were rescaled so that the probability that a parasite switches to another or the same variant is 0.01 per population doubling. (*Middle*) Black lines represent the total number of parasites, and each colored line represents a variant. (*Bottom*) Shown is the immune response against each variant. Simulations began with 1,000 trypanosomes and a repertoire of 30 *VSG*s. Because this is a small proportion of the potential *in vivo* repertoire (≈2,000 *VSG*s), duration of simulated infections is much briefer than occurs *in vivo*. Parameters are the same as in Fig. 2. (*A*) All variants are chosen from the same distribution. (*B*) Fifteen of the variants are chosen from the left-hand distribution, and 15 are chosen from the right-hand distribution. (*C*) Ten variants are chosen from each of the three distributions.

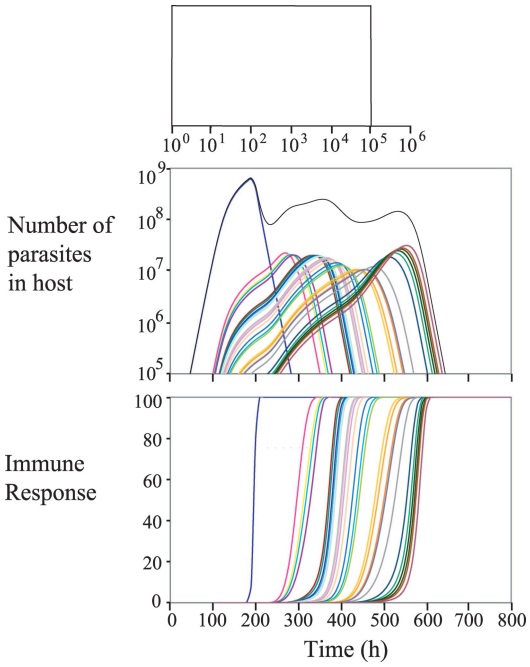

Fig. 4. Time series of the parasite dynamics and the immune response with a homology-based switching pattern. The rate to which a *VSG* is switched depends on its homology with the *VSG* that it is replacing. It is assumed (12, 13) that *VSG*s with the closest homology are more likely to switch to each other. For example, *VSG*s 1 and 2 have very high homology, whereas 1 and 30 have the lowest homology. A total of 30 switching rates were chosen randomly from the distribution shown at the top. The highest switching rate determines the rate at which a variant switches to itself, $s_{i,i}$. The next highest switching rate determines the rate at which *VSG*s with the closest homology switch to each other, $s_{i,i(\pm)1}$, and so on. Once all the switching rates are chosen, they are rescaled so that the probability that a parasite switches to another or the same variant is 0.01 per population doubling. Parameters used are the same as in Fig. 2.

When modeling the impact of the immune response on infection dynamics, it is most important to capture the dynamics of parasite removal, which can be done without making detailed assumptions about underlying mechanisms. Because the kinetics of antibody production and variant killing strongly correlate, it is antibody empirical data on which we base the model. We modeled the acquired immune response, a_i, by using a single equation,

$$\frac{da_i}{dt} = c_i(1 - a_i)\left(\frac{v_i' + m_i'}{C}\right)^x, \qquad [5]$$

where c_i (which determines the maximum rate at which the immune response can increase against variant i), C (a scaling factor), and x (rate of growth of the response) are constants, and the prime indicates the number of cells at time $t - \tau$, where τ is the time it takes for the immune system to respond. For all simulations, $c_i = 100$ and $C = 1 \times 10^8$. The immune response against variant i grows at an intrinsic rate determined by the number of cells of variant i. The intrinsic growth rate of the immune response x leads to a threshold of effectiveness, above which there is killing of the parasite, as occurs *in vivo* (46, 47). Whether trypanosomes can resist antibodies during switching or at low antibody levels (24, 48) would be included in these empirical profiles of immunity and do not need to be factored. Another generality on the basis of evidence (14, 15) is that immune responses are very persistent.

Results

To establish the basic behavior of the model independently of differential switching, initially we incorporated a uniform switching pattern (Fig. 1*A*) in which the probability of switching to another (or the same) variant and the probability of each of the variants being switched on is 0.01 per population doubling (49). One consequence of switching is that there is constant regeneration of previously expressed variants and their rapid elimination by existing antibodies. This regeneration is included in our model but has a negligible effect on overall population dynamics, because only 1% of the population is switching at any time, and therefore only 1% of the population is potentially vulnerable to these existing antibodies at any time. As expected, the *VSG* repertoire is quickly exhausted, there is no order in expression, and the infection is quickly eliminated by the host immune system (Fig. 2). To investigate the effect of differential switching, we next assumed the differential-activation pattern shown in Fig. 1*C*. Because the activation rate of each variant is independent of the currently expressed variant, the value of $s_{i,j}$ depends only on i and not on j (so, for example, $s_{1,1} = s_{1,2} = s_{1,3}$ and so on). Initially, we incorporated switch rates from a continuous range, from high to low activation probability, with a range of nearly 100,000-fold in the activation rates of different variants (once chosen, the switch rates remain constant throughout the simulation). This range may or may not reach the lowest *VSG* switch rate, which is unknown, but a wider range of activation probabilities would simply extend the chronicity of infection. Fig. 3*A* reveals order in variants and in the corresponding immune responses. During the first peak of parasitemia, the inoculated variant type predominates, with different variants being generated continually, according to their inherent activation rate. The first immune response removes the infecting variant, allowing the next variant to become more predominant, and the cycle of growth and death repeats for all variants. Superimposed on this is higher-level fluctuation of the whole parasitemia, resulting from the density-dependent differentiation from long slender to short stumpy, nondividing, stage (34). The general features of these initial simulations resemble what occurs *in vivo* (15, 16): no variants reappeared, there was positive correlation between the activation time of each variant and the appearance of a strong antibody response, many variants were present simultaneously, and the parasitemia occurred in waves. Thus, differential activation probabilities clearly can be a major factor in determining order, which does not require a complex switch matrix in which the activation probability depends on the VSG being expressed.

We then tested whether discontinuous switch rate changes, corresponding to the early and later groups *in vivo* (16), yield realistic patterns of antigenic variation and parasitemia. Using the differential-activation switching pattern (Fig. 1*C*), we included a faster and a slower group of 15 variants each for the second set of simulations (Fig. 3*B*). The third set of simulations included 10 variants each assigned to high, medium, and low activation probabilities (Fig. 3*C*). Both the second and third sets of simulations produced more distinct parasitemia peaks and more prominent variant subpeaks (Fig. 3 *B* and *C*) than the first set of simulations (Fig. 3*A*). As the number of switch rate distributions increases, there is a progressive clustering of the variant-specific immune responses, tending toward what has been observed to occur *in vivo* (15, 32, 50).

To examine the influence of mosaic-activated switching, whereby the extent of homology with the coding sequence of the active *VSG* determines likelihood of participation in the switch, we modeled it in isolation, with the assumptions that switching is reversible and that *VSG* 1 was most homologous to 2, which in turn was most and equally homologous to 1 and 3, etc. ($s_{i,j} = s_{j,i}$ for all i and j) (Fig. 1*D*). Our simulations of homology-based

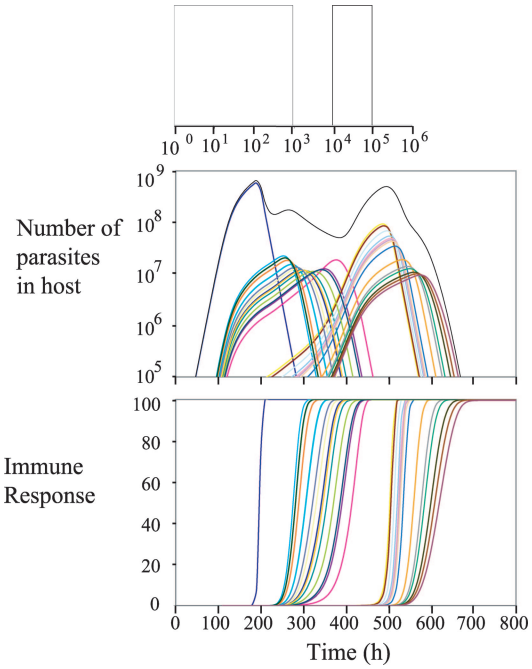

Fig. 5. Time series of the parasite dynamics and the immune response in which there are two classes of variant, those with a differential activation switching pattern and those with a homology switching pattern. The homology of the 30 *VSG*s was determined by randomly drawing switch rates from the left-hand distribution shown at the top. Fifteen of these variants were then randomly allocated to the class of variants whose switch rate is independent of which variant they are replacing. Their switch rates were randomly chosen from the right-hand distribution. Parameters used are the same as in Fig. 2.

switching yield, within each relapse peak, several variant subpeaks and ordered progression (Fig. 4). Finally, to model the *in vivo* situation, we combined differential-activation and homology-dependent switching (Fig. 1 *C* and *D*). Fifteen variants were allocated to each switch mechanism (Fig. 5), with the flank-activated *VSG*s having an activation rate between one and five orders of magnitude higher than the mosaic *VSG*s. These simulations produce the same general features as both previous series and patterns strongly resembling what occurs *in vivo* (32).

Discussion

It is clear from all of the discontinuous rate range simulations (Figs. 3–5) that intrinsic *VSG* activation rates can provide order in antigenic variation and that the switching distribution has a strong influence on antigenic variation patterns. A patent prediction is that the characteristic groupings of variants in each parasitemia peak *in vivo* (15, 16) arise primarily from the existence of discontinuous switch ranges. Superimposed on this primary effect are the combined effects of density-dependent differentiation to the stumpy stage and immune responses, which result in aggregation of more variants within growth peaks and greater spacing between peaks. A challenge is to search for these putative *VSG* groupings, which are on a finer scale than those proposed by Capbern *et al.* (16), and then to determine their molecular basis.

Thus, two main factors, both parasite-determined, can account for ordered antigenic variation in chronic infection. They are simple variation in activation rates and differentiation to the nondividing transmission stage. Our model is thus more parsimonious than previous theoretical models and more consistent with experimental data (see above). It can be argued that both differential activation probabilities and density-dependent differentiation apply generally to antigenic variation in eukaryotic parasites. Stochastic, ordered switching is held to be common to bacterial and eukaryotic pathogens (51, 52). Density-dependent differentiation to a nondividing stage, although not evident in bacteria, is well documented in eukaryotic parasites. An interesting case is *Giardia*, which encysts with density dependence and appears to produce new antigenic variants upon excystation (53). Nevertheless, trypanosome antigenic variation differs from that of other pathogens in its likely scale, the repertoire consisting of up to 2,000 *VSG* genes, the majority of which are pseudogenes. In contrast, the silent MSP2 archive of the bacterium *Anaplasma marginale* comprises just five pseudogenes (6), whereas the *P. falciparum var* archive has ≈60 members (54). The trypanosome archive may have enlarged so much because, unlike the variable antigens of other pathogens, the VSG appears not to have biochemical function, presumably allowing more unrestrained, diversifying evolution. The combinatorial use of damaged genes to create novel, expressed mosaic genes can greatly enlarge the effective archive, as seen with *A. marginale* (6), so *T. brucei* theoretically has strikingly enormous potential, with corresponding capability for lengthening infection (55).

There may be two reasons for the possible silent information overload. One is that African trypanosomes live permanently extracellularly in the vasculature, provoking extensive antibody responses. The other relates to rate of archive use. In our analysis, the experimental set of 30 *VSG*s was expended in only two or three peaks. This is more profligate than generally has been concluded from empirical clonal studies, but those studies screened only a few selected VSGs, in unusually slowly switching strains (14, 22, 36). Nevertheless, profligacy of similar magnitude has been recorded in the first relapse after the more natural situation, tsetse fly transmission (56). It might be concluded that trypanosome antigenic variation appears effectively to be pitched in a war of attrition with the host antibody responses, the two systems attempting to match the rapid diversification of each other. By simple force of numbers, trypanosome antigenic variation apparently does not require the subtleties, such as transient cross-reactive immune responses, that have been hypothesized for *Plasmodium* (30). An important consequence of order being determined by the trypanosome, rather than the host, is that distinct series, or "strings," of variants can be generated in different infections with the same strain because of the stochastic nature of mosaic gene formation. Such dissimilarity between infections might enable effective transmission in the face of herd immunity (57).

We thank Sean Nee for discussions and the Wellcome Trust for funding. J.D.B. is a Wellcome Trust Principal Research Fellow.

1. Berriman M, Ghedin E, Hertz-Fowler C, Blandin G, Renauld H, Bartholomeu DC, Lennard NJ, Caler E, Hamlin NE, Haas B, *et al.* (2005) *Science* 309:416–422.
2. Thon G, Baltz T, Eisen H (1989) *Genes Dev* 3:1247–1254.
3. Steinert M, Pays E (1985) *Br Med Bull* 41:149–155.
4. Borst P (1986) *Annu Rev Biochem* 55:701–732.
5. Pays E (1989) *Trends Genet* 5:389–391.
6. Futse JE, Brayton KA, Knowles DP, Palmer GH (2005) *Mol Microbiol* 57:212–221.
7. Young JR, Shah JS, Matthyssens G, Williams RO (1983) *Cell* 32:1149–1159.
8. Laurent M, Pays E, Van der Werf A, Aerts D, Magnus E, Van Meirvenne N, Steinert M (1984) *Nucleic Acids Res* 12:8319–8328.
9. Myler PJ, Allison J, Agabian N, Stuart KD (1984) *Cell* 39:203–211.
10. Liu AYC, Michels PAM, Bernards A, Borst P (1985) *J Mol Biol* 182:383–396.
11. Van der Werf A, Van Assel S, Aerts D, Steinert M, Pays E (1990) *EMBO J* 9:1035–1040.
12. Thon G, Baltz T, Giroud C, Eisen H (1990) *Genes Dev* 4:1374–1383.
13. Kamper SM, Barbet AF (1992) *Mol Biochem Parasitol* 53:33–44.
14. Robinson NP, Burman N, Melville SE, Barry JD (1999) *Mol Cell Biol* 19:5839–5846.

15. Morrison LJ, Majiwa P, Read AF, Barry JD (2005) *Int J Parasitol* 35:961–972.
16. Capbern A, Giroud C, Baltz T, Mattern P (1977) *Exp Parasitol* 42:6–13.
17. Barry JD (1986) *Parasitology* 92:51–65.
18. Seed JR (1978) *J Protozool* 25:526–529.
19. Aslam N, Turner CMR (1992) *Parasitol Res* 78:661–664.
20. Kosinski RJ (1980) *Parasitology* 80:343–357.
21. Agur Z, Abiri D, Van der Ploeg LHT (1989) *Proc Natl Acad Sci USA* 86:9626–9630.
22. Van Meirvenne N, Janssens PG, Magnus E (1975) *Ann Soc Belg Med Trop* 55:1–23.
23. Munoz-Jordan JL, Davies KP, Cross GAM (1996) *Science* 272:1795–1797.
24. Dubois ME, Demick KP, Mansfield JM (2005) *Infect Immun* 73:2690–2697.
25. Antia R, Nowak MA, Anderson RM (1996) *Proc Natl Acad Sci USA* 93:985–989.
26. Agur Z, Mehr R (1997) *Parasite Immunol (Oxf)* 19:171–182.
27. Jackson DG, Windle HJ, Voorheis HP (1993) *J Biol Chem* 268:8085–8095.
28. Ziegelbauer K, Overath P (1993) *Infect Immun* 61:4540–4545.
29. Radwanska M, Magez S, Dumont N, Pays A, Nolan D, Pays E (2000) *Parasite Immunol (Oxf)* 22:639–650.
30. Recker M, Nee S, Bull PC, Kinyanjui S, Marsh K, Newbold C, Gupta S (2004) *Nature* 429:555–558.
31. Vervoort T, Barbet AF, Musoke AJ, Magnus E, Mpimbaza G, Van Meirvenne N (1981) *Immunology* 44:223–232.
32. Gray AR (1965) *J Gen Microbiol* 41:195–214.
33. Reuner B, Vassella E, Yutzy B, Boshart M (1997) *Mol Biochem Parasitol* 90:269–280.
34. Tyler KM, Higgs PG, Matthews KR, Gull K (2001) *Proc R Soc London Ser B* 268:2235–2243.
35. Frank SA (1999) *Proc R Soc London SerB* 266:1397–1401.
36. Miller EN, Turner MJ (1981) *Parasitology* 82:63–80.
37. Turner CMR, Aslam N, Angus SD (1996) *Parasitol Res* 82:61–66.
38. Mansfield JM, Paulnock DM (2005) *Parasite Immunol (Oxf)* 27:361–371.
39. Turner CM, Hunter CA, Barry JD, Vickerman K (1986) *Trans R Soc Trop Med Hyg* 80:824–830.
40. Sternberg JM (2004) *Parasite Immunol (Oxf)* 26:469–476.
41. Doyle JJ, Hirumi H, Hirumi K, Lupton EN, Cross GAM (1980) *Parasitology* 80:359–369.
42. Seed JR, Effron HG (1973) *Parasitology* 66:269–278.
43. Hertz CJ, Filutowicz H, Mansfield JM (1998) *J Immunol* 161:6775–6783.
44. Turner CMR, Aslam N, Dye C (1995) *Parasitology* 111:289–300.
45. McLintock LL, Turner CR, Vickerman K (1993) *Parasite Immunol (Oxf)* 15:475–480.
46. Morrison WI, Black SJ, Paris J, Hinson CA, Wells PW (1982) *Parasite Immunol (Oxf)* 4:395–407.
47. Morrison WI, Murray M (1985) *Parasite Immunol (Oxf)* 7:63–79.
48. Pal A, Hall BS, Jeffries TR, Field MC (2003) *Biochem J* 374:443–451.
49. Turner CMR, Barry JD (1989) *Parasitology* 99:67–75.
50. Barry JD, Emery DL (1984) *Parasitology* 88:67–84.
51. Handunnetti SM, Mendis KN, David PH (1987) *J Exp Med* 165:1269–1283.
52. Frank SA, Barbour AG (2006) *Infec Genet Evol* 6:141–146.
53. Svard SG, Meng TC, Hetsko ML, McCaffery JM, Gillin FD (1998) *Mol Microbiol* 30:979–989.
54. Kraemer SM, Smith JD (2003) *Mol Microbiol* 50:1527–1538.
55. Marcello L, Barry JD (2007) *J Eukaryot Microbiol*, 54:14–17.
56. Hajduk SL, Vickerman K (1981) *Parasitology* 83:609–621.
57. Barry JD, Marcello L, Morrison LJ, Read AF, Lythgoe K, Jones N, Carrington M, Blandin G, Bohme U, Caler E, *et al.* (2005) *Biochem Soc Trans* 33:986–989.